

# Novel Oral mTORC1/2 Inhibitor TAK-228 Has Synergistic Antitumor Effects When Combined with Paclitaxel or PI3K $\alpha$ Inhibitor TAK-117 in Preclinical Bladder Cancer Models



Anna Hernández-Prat<sup>1</sup>, Alejo Rodríguez-Vida<sup>1,2</sup>, Nuria Juanpere-Rodero<sup>1,3,4</sup>, Oriol Arpi<sup>1</sup>, Silvia Menéndez<sup>1</sup>, Luis Soria-Jiménez<sup>1</sup>, Alejandro Martínez<sup>1,2</sup>, Natalia Iarchouk<sup>5</sup>, Federico Rojo<sup>6</sup>, Joan Albanell<sup>1,2,4</sup>, Rachael Brake<sup>5</sup>, Ana Rovira<sup>1,2</sup>, and Joaquim Bellmunt<sup>1,2,7</sup>

## Abstract

Advanced bladder cancer is associated with a poor prognosis and limited treatment options. The PI3K/AKT/mTOR pathway is frequently activated in this disease and can be a potential therapeutic target for treatment intervention. We studied the antitumor efficacy of a new targeted therapy, TAK-228 (oral mTORC1/2 inhibitor), in preclinical models of bladder cancer. We evaluated the effects of TAK-228 in combination with a PI3K $\alpha$  inhibitor (TAK-117) or with chemotherapy (paclitaxel). We used six bladder cancer cell lines and *in vivo* xenografts models. TAK-228 strongly inhibited cell proliferation *in vitro*, and reduced tumor growth and angiogenesis *in vivo*. Three possible biomarkers of response to TAK-228 (basal levels of 4E-BP1, p-4E-BP1/4E-BP1 ratio, or eIF4E/4E-BP1 ratio) were identified. The combination of TAK-228 and TAK-117 had synergistic effects *in vitro* and *in vivo*. Furthermore, TAK-228 demon-

strated greater efficiency when combined with paclitaxel. TAK-228 also showed *ex vivo* activity in tumor tissue from patients with treatment-naïve bladder cancer. TAK-228 is a promising investigational agent that induces a strong effect on cell proliferation, tumor growth, and angiogenesis in bladder cancer models. High synergistic effects were observed with TAK-228 combined with a PI3K inhibitor or with chemotherapy. These results are currently being investigated in a clinic trial of TAK-228 plus paclitaxel in patients with metastatic bladder cancer (NCT03745911).

**Implications:** Strong synergistic effects were observed when combining TAK-228 with TAK-117 (a PI3K $\alpha$  inhibitor) or with paclitaxel chemotherapy. A phase II study at our institution is currently evaluating the efficacy of TAK-228 combined with paclitaxel in patients with metastatic bladder cancer.

## Introduction

Bladder cancer is a major source of mortality worldwide, with an estimated 79,000 new cases and 17,000 deaths in the United States in 2017 (1). When it is diagnosed at an early localised stage, radical cystectomy is the standard-of-care treatment. For patients who relapse after surgery or for *de novo* metastatic patients, palliative platinum-based chemotherapy is the recommended

therapy. Until 2017, following disease progression to first-line chemotherapy, there was no internationally accepted standard second-line regimen, with vinflunine chemotherapy, being only approved in Europe after showing modest results in a phase III trial (2). In 2017, several immune checkpoint inhibitors targeting the programmed cell death-1 (PD-1) pathway showed clinically relevant signs of antitumor activity in patients with advanced bladder cancer. Pembrolizumab, a PD-1 inhibitor, showed for the first time, an improvement in overall survival compared with standard chemotherapy in the second-line setting (3). Monotherapy with other immune checkpoint inhibitors has also shown promising results (4). The objective response rate in these studies ranged from 15% to 20%, which indicates that a significant proportion of patient does not benefit from immunotherapy. Despite the significant duration of response observed with these agents, some patients will ultimately experience disease progression. Therefore, therapies for improving the outcome of patients with advanced bladder cancer are needed.

Detailed molecular information on bladder cancer is now available thanks to the Cancer Genome Atlas (5). However, no targeted agents have been approved for advanced bladder cancer treatment. Several antiangiogenic agents and anti-EGFR-targeted therapies were investigated but showed no significant clinical benefit in clinical trials (6). FGFR inhibitors are emerging as a potential target but results from randomized trials are awaited (7).

<sup>1</sup>Cancer Research Program, IMIM (Hospital del Mar Research Institute), Barcelona, Spain. <sup>2</sup>Medical Oncology Department, Hospital del Mar-CIBERONC, Barcelona, Spain. <sup>3</sup>Pathology Department, Hospital del Mar-CIBERONC, Barcelona, Spain. <sup>4</sup>Medical School, Universitat Pompeu Fabra (UPF), Barcelona, Spain. <sup>5</sup>Millennium Pharmaceuticals, Inc., Cambridge, Massachusetts. <sup>6</sup>Pathology Department, IIS-Fundación Jiménez Díaz, Madrid, Spain. <sup>7</sup>Dana-Farber/HCC, Harvard Medical School, Boston, Massachusetts.

**Note:** Supplementary data for this article are available at Molecular Cancer Research Online (<http://mcr.aacrjournals.org/>).

**Corresponding Author:** Joaquim Bellmunt, IMIM (Hospital del Mar Research Institute), PRBB Building, Doctor Aiguader, 88, 1st Floor (office 100.06.02), Barcelona 08003, Spain. Phone: 34-93-316-0750; Fax: 34-93-316-0410; E-mail: jbellmunt@imim.cat

Mol Cancer Res 2019;17:1931-44

doi: 10.1158/1541-7786.MCR-18-0923

©2019 American Association for Cancer Research.

PI3K/AKT/mTOR pathway is frequently altered in cancer (8) and is a potential therapeutic target. This pathway plays a critical role in relevant cellular processes such as cell proliferation, survival, apoptosis, and metabolism (8, 9). PI3K, Akt (a serine/threonine kinase also named PKB), and mTOR are the three major players of this pathway (9) with almost 50% of bladder cancer s showing alterations in this pathway (10, 11). E542K, E545K, and H1047R are the most common activating point mutations of the p110 $\alpha$  catalytic subunit of PI3K (*PI3KCA*). In addition, mutations or inactivating deletions in the *TSC1* gene are also prevalent (10, 11) and are associated with increased mTORC1 activity (12). Finally, several alterations in 4E-BP1 and eIF4E have been correlated with an impaired outcome in patients with bladder cancer (13, 14). These frequent molecular alterations make the PI3K/AKT/mTOR pathway an attractive pathway to target in patients with bladder cancer.

Preclinical studies have showed that everolimus (mTORC1 inhibitor) is active in selected bladder cancer models, both *in vitro* and *in vivo* (12, 15, 16). However, despite these preclinical effects, everolimus and the rapalogs have, in general, very limited efficacy when given as monotherapy to patients (12). The activity of many other small molecules inhibiting other key nodes (PI3K and AKT) in the pathway has been also preclinically studied in bladder cancer (17, 18).

The new dual mTOR kinase inhibitors are ATP-competitive inhibitors that bind to the catalytic site and potently suppress both mTORC1 and mTORC2 kinase activity. Importantly, these agents are more effective than rapalogs in inhibiting the pathway. mTORC1/2 inhibitors such as PP242, OSI-027, and Torin1 have demonstrated superior antitumor effects than rapamycin in several cancer models including bladder cancer (19–21). TAK-228 (sapanisertib) is an orally bioavailable, potent, and highly selective mTORC1/2 inhibitor that inhibits growth of human cell lines of various cancer types (22–26). Until very recently, its activity in bladder cancer models has not been well characterized (27). So far no mTORC1 inhibitor has shown clinical activity in unselected patients with advanced bladder cancer. Consequently dual mTOR inhibitors such as TAK-228 are currently being tested in patients to assess whether they are associated with greater clinical efficacy. In this article, we aim to characterize the effects of TAK-228, as single agent or combined with TAK-117, an upstream PI3K inhibitor, or with paclitaxel, looking for potential synergistic effects in bladder cancer cell lines with different genomic alterations. These combinations were also tested in several cell line–derived xenografts and *ex vivo* in tumor explants obtained from patients with treatment-naïve bladder cancer. Finally, we aimed to identify molecular predictive biomarkers of response that could potentially help in better selecting patients for future biomarker-driven clinical trials.

## Materials and Methods

### Cell culture

Human bladder cancer cell lines obtained from ATCC (T24, HT-1197, TCCSUP, UM-UC-3, and RT4) or from DSMZ (CAL-29) were grown in Minimum Essential Medium supplemented with L-glutamine (2 mmol/L/L), penicillin/streptomycin (100 U/100  $\mu$ g/mL; Live Technologies), and 10% FBS (Sigma-Aldrich) and maintained at 37°C under a 5% CO<sub>2</sub> humidified atmosphere. The absence of *Mycoplasma* contamination in cell cultures was assessed following the standard operative procedures of our institution, as described previously (28). The number of

passages between the described experiments was twenty or less. At the end of the study, cell lines were authenticated using short-tandem repeat DNA profiling recommended by ATCC experts.

### Reagents

TAK-228 and TAK-117 were provided by Millennium Pharmaceuticals. Everolimus and paclitaxel were from Selleckchem. For *in vitro* studies, 10 mmol/L DMSO stock solutions were stored at –20°C. For *in vivo* studies, TAK-228 and TAK-117 were prepared in PEG400 as described by the manufacturer and stored at room temperature 1 week. Paclitaxel (from Teva) was prepared in physiologic serum.

### Viability assays

Cells (1,000–7,000 cells/well) were seeded depending on their doubling time in 96-well flat-bottom plates. For the three-dimensional (3D) cultures, 5,000 cells were seeded in round-bottom ultra-low attachment 96-well plates and centrifuged for 10 minutes at 1,000  $\times$  g. Next day, cells and 3D-spheroids were treated as indicated for 72 hours. Cell viability was measured by the MTS CellTiter 96 AQ One solution Cell proliferation assay (2D cultures) or CellTiter-Glo Luminescent cell viability assay (3D cultures; Promega). In some experiments, cells were trypsinized, diluted, and counted by an automatic cell counter (Scepter, Millipore).

### Western blotting analysis

Western blots were performed according to standard protocols. Cells were plated in 100-mm<sup>2</sup> dishes and after 24 hours cells were treated as indicated for each experiment. The following antibodies were used: p-Akt (Ser473), p-Akt (Thr308), Akt, p-S6 (Ser235/236), S6, p-4E-BP1 (Thr37/46), 4E-BP1, eIF4E, p-eIF4E (Ser209) LC3-I-II, p62/SQSTM1, cleaved-PARP, Cyclin D1 and TSC1 (Cell Signaling Technology),  $\alpha$ -tubulin (Sigma-Aldrich), and GAPDH (Santa Cruz Biotechnology). Mouse and rabbit horseradish peroxidase (HRP)-conjugated secondary antibodies (GE Healthcare Life Sciences) were used. The anti- $\alpha$ -tubulin or GAPDH antibodies were used as control to verify equal protein loading across samples. Bands were measured using QuantityOne software. In all the Figures, representative blots from three independent experiments are shown.

### Cell cycle and apoptosis

Cells were seeded in 100-mm<sup>2</sup> dishes and after 24 hours cells were treated with the drugs. For cell-cycle analysis, cells were fixed during 3 days and stained with propidium iodide for 30 minutes and analyzed by flow cytometry (FACSCalibur). Apoptosis was analyzed by Muse Cell Analyzer (Millipore) using the Annexin V and Dead Cell Assay Kit (Millipore) and analyzed with MuseSoft 1.4.0.0.

### Autophagy

Cells were seeded on tissue culture slides and after 24 hours, they were treated with the drugs. Cells were stained with Microscopy Dual Detection Reagent (Enzo Life Sciences) and analyzed by fluorescence microscopy according to the manufacturer's protocol. Autophagy was also analyzed by Western blot.

### Establishment of tumor xenografts in nude mice

All animal work was conducted following the PRBB Institutional Animal Care and Scientific Committee guidelines.

Five-week-old male BALB/c nude mice were subcutaneously inoculated in their flank with  $5 \times 10^6$  RT4 cells,  $20 \times 10^6$  CAL-29 cells, or  $1.5 \times 10^6$  UM-UC-3 cells mixed with Matrigel. Tumor growth was measured twice a week. Mean tumor volume at the experiment initiation was around  $200 \text{ mm}^3$  based on our previous experience (29) and published reports. Treatment is given to the mice when the tumor volume is in the range of 75 to  $350 \text{ mm}^3$ . Mice were distributed homogeneously into experimental groups. Treatment groups are described in figure legends. TAK-228 and TAK-117 (oral gavage) and paclitaxel (intraperitoneal) were administered according to a preestablished dosing regimen. Animals were sacrificed at the various times indicated postdose, and tumor tissue was harvested frozen at  $-80^\circ\text{C}$  or in formalin-fixed paraffin-embedded (FFPE).

#### Ex vivo treatment of fresh tumor samples

We used two types of samples: cell line-derived xenograft and human tumor tissue from patients with bladder cancer. The latter were obtained following IRB approval (2016/6767/1) from transurethral resection of the bladder in 6 previously untreated patients with bladder cancer. *Ex vivo* assays were performed according to our own experience (30). Briefly, fresh tumor samples were immediately sliced and cultured with or without the drug as indicated. Samples were FFPE and analyzed by IHC.

#### IHC

FFPE blocks were cut in  $5\text{-}\mu\text{m}$  tissue sections and were immunostained in a Dako Link platform. The final H-score value (the percentage of cells at each staining intensity) or the percentage of positive tumor cells for each case was determined according to our own experience (30). The antibodies used were as follows: pH3, p-S6 (Ser235/236), VEGF-A, cleaved caspase-3 (Cell Signaling Technology), and CD31 (Spring Bioscience).

#### Statistical analysis

Statistical analysis was carried out with SPSS version 18.0 (SPSS, Inc.). Student *t* test or ANOVA were used for comparisons between groups. Nonlinear (polynomial) regression was used for the viability assay (dose-response curve). To test for correlation, we used the Spearman rank correlation coefficient (*r*). We considered correlation when *r* was close to  $\pm 1$ . Results were considered significant when  $P < 0.05$ .

## Results

### TAK-228 decreases cell proliferation in a dose-dependent manner

We tested the antiproliferative effects of TAK-228 in 6 bladder cancer cell lines with different underlying genetic background in *PI3KCA*, *TSC1/2*, *PTEN*, and *RAS* genes according to the Cosmic Catalog of Somatic Mutations in Cancer and the Broad-Novartis Cancer Cell Line Encyclopedia (Supplementary Table S1; ref. 31). We did not find evidences of *EIF4EBP1* or *EIF4E* mutations in these cells. TAK-228 reduced the proliferation of all bladder cancer cells in a concentration-dependent manner with  $\text{IC}_{50}$  values ranging from 24 to  $41.6 \text{ nmol/L}$  (Fig. 1A). RT4 cells (*TSC1*-mutant) were significantly more sensitive than other cell lines ( $P < 0.001$ ; Fig. 1A).

### TAK-228 arrests cell cycle and induces apoptosis and autophagy

The inhibitory effects of TAK-228 on cell proliferation prompted us to evaluate its effects in modulating cell cycle, apoptosis, and autophagy. We used the RT4 and CAL-29 cell lines, the two most sensitive cells. In RT4 cells, TAK-228 significantly increased the number of cells in  $G_0\text{-}G_1$  phase and reduced the cells in S phase ( $P < 0.05$ ). Similarly, the quantity of cells in  $G_2\text{-}M$  phase was decreased. Same trend was observed in CAL-29 cells, despite the differences not being significant (Fig. 1B).

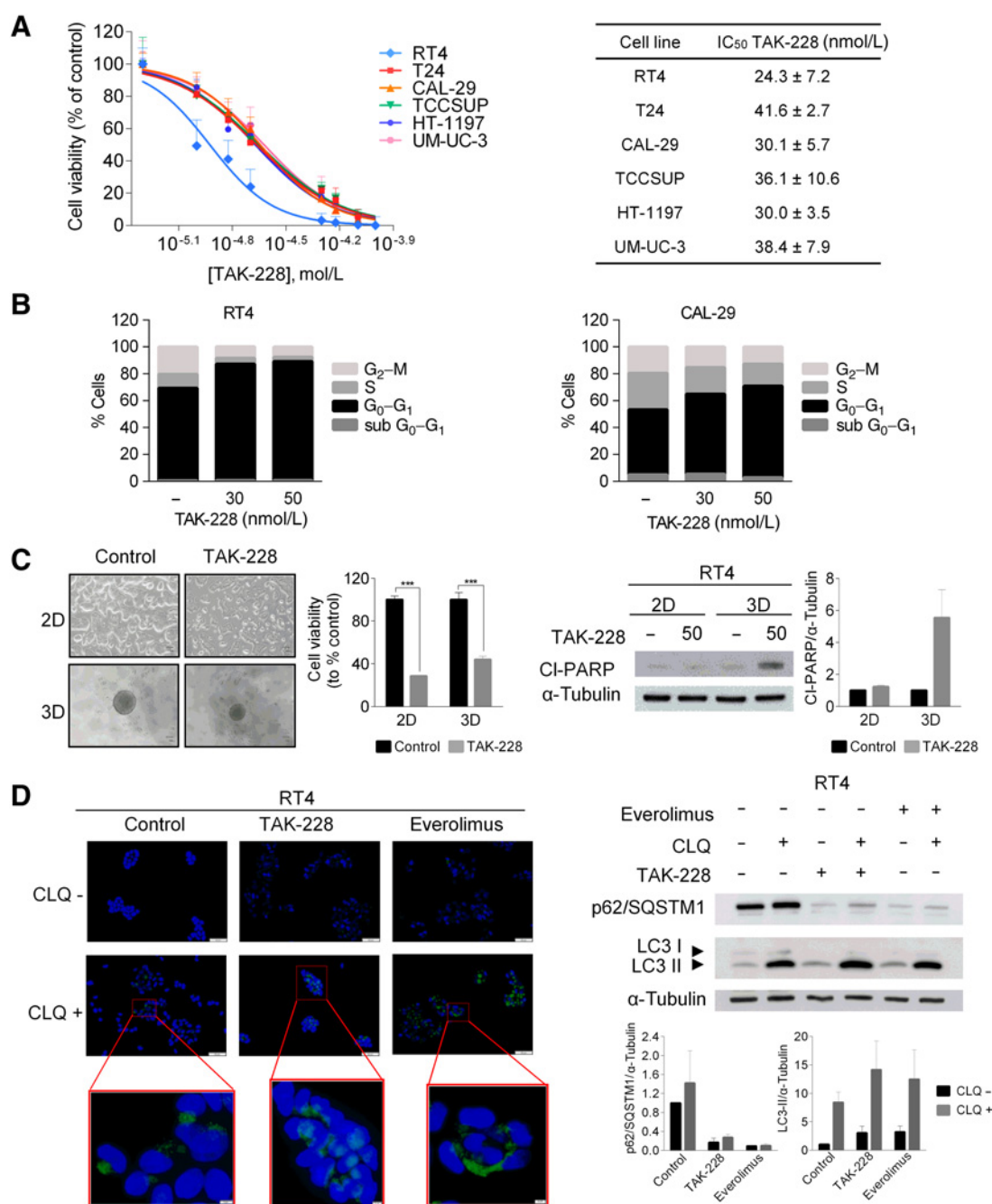
As TAK-228 induces apoptosis in breast and colon cancer cells *in vitro* (22, 26), we analyzed whether TAK-228 was also able to induce apoptosis in bladder cancer cells. We treated the cells with TAK-228 during 48 hours and no apoptosis effect was detected through Western blot analysis (cleaved-PARP) and Muse Cell Analyzer using the Muse AnnexinV & dead cell kit (Supplementary Fig. S1A). Apoptosis was not observed when extending treatment for 3 days or when performing high-dose experiments (Supplementary Fig. S1A). Contrary, when we evaluated the effects of TAK-228 in a 3D spheroid model that better mimics the tumor characteristics *in vivo* (32), we found that TAK-228-treated RT4 spheroids undergo apoptosis as early as 24 hours posttreatment (Fig. 1C).

It has been reported that classical mTOR inhibitors and dual mTORC1/2 inhibitors induce autophagy (33, 34). We checked through Western blot the levels of two proteins involved in autophagy: LC3-II and p62/SQSTM1. We demonstrated that TAK-228 decreases the levels of p62 and increases the levels of LC3-II in RT4 and CAL-29 cells (Fig. 1D; Supplementary Fig. S1B, respectively). A high accumulation of autophagic vesicles in RT4 cells was detected with fluorescence microscopy after treatment with TAK-228 (Fig. 1D). On the basis of these results, we can conclude that TAK-228 induces cell-cycle arrest in  $G_0\text{-}G_1$  phase and activates autophagy and apoptosis on the tested cells.

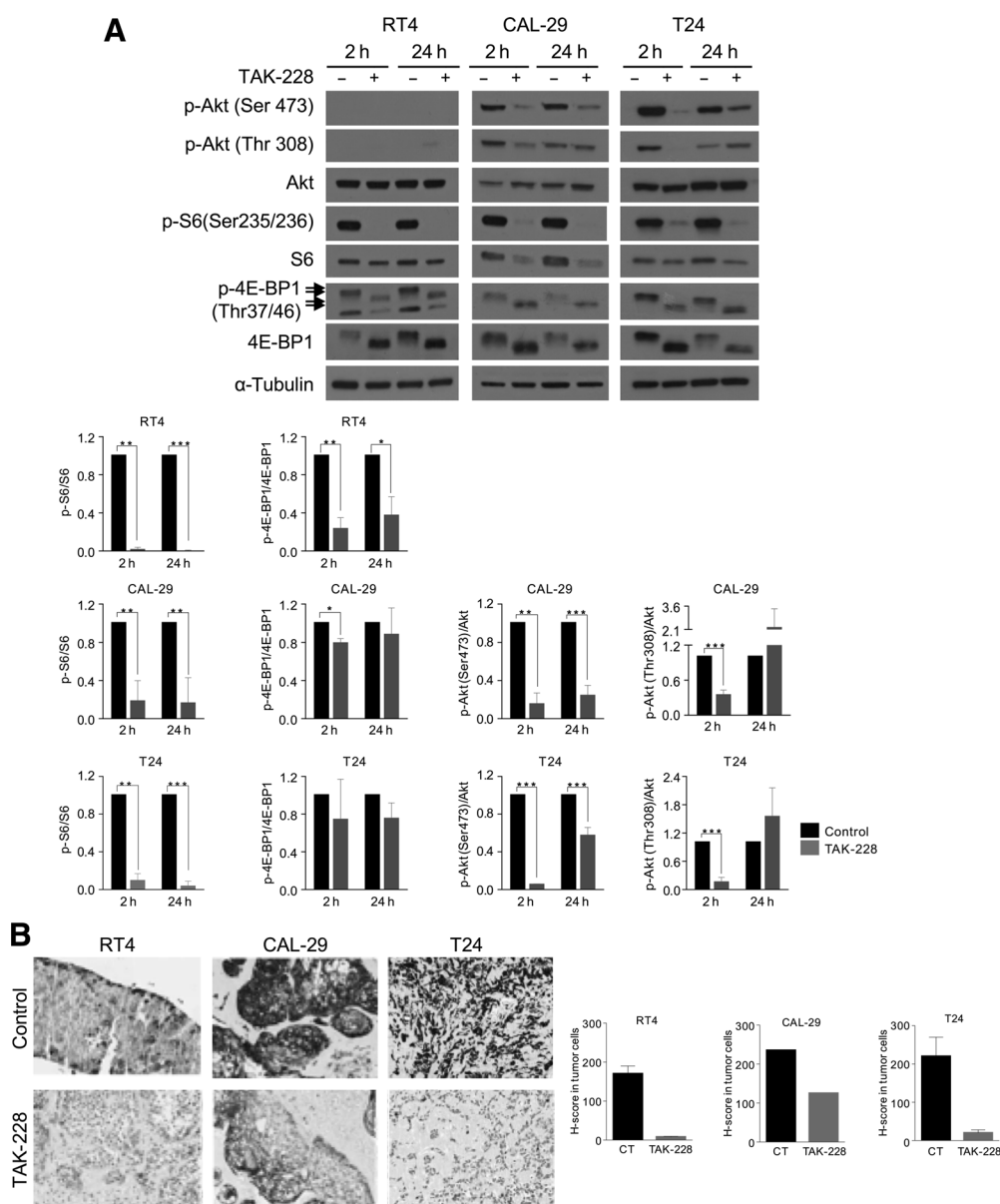
### TAK-228 inhibits PI3K/AKT/mTOR pathway

We evaluated the inhibitory effects of TAK-228 on the PI3K/AKT/mTOR pathway by Western blot analysis in CAL-29, T24, and RT4 cell lines. To assess the effects of TAK-228 on mTORC2, we analyzed the AKT activation through phosphorylation at the Ser473 site (Fig. 2A). TAK-228 inhibited the phosphorylation of AKT at Ser473 in CAL-29 and T24 cells at 2 and 24 hours. AKT phosphorylation at Ser473 was almost recovered at 24 hours in T24 cells but not in CAL-29. AKT phosphorylation at Thr308 was inhibited at 2 hours but had recovered at 24 hours in both T24 and CAL-29. Phosphorylation of AKT was not observed in RT4 at basal conditions. Total AKT levels were unchanged after treatment of these three cell lines.

Phosphorylation of S6, a direct downstream target of mTORC1, was found to be completely abolished by TAK-228 2 hours after treatment and this effect was maintained for 24 hours in the three tested cell lines. Total S6 levels decreased slightly after drug treatment. In addition, TAK-228 significantly reduced the phosphorylation of 4E-BP1 Thr37/46, (downstream of mTORC1) in RT4 cells (Fig. 2A), in a dose-dependent way (data not shown). There was also a slight decrease of 4E-BP1 phosphorylation in CAL-29 and T24 (Fig. 2A). We compared with the mTORC1 inhibitor everolimus and inhibition of S6 phosphorylation but not of AKT or 4E-BP1 (Supplementary Fig. S2) was observed, suggesting that TAK-228 is more effective than everolimus on inhibiting the PI3K pathway.

**Figure 1.**

Cellular effects of TAK-228 on human bladder cancer cell lines *in vitro*. **A**, Effects of TAK-228 on cell viability. Cells were treated with increasing doses of TAK-228 (5, 10, 15, 20, 50, 60, 80, 100 nmol/L; six-well each) for 72 hours. Cell viability was determined using MTS assay. Values shown are the mean percentage  $\pm$  SD of cell viability relative to controls and plotted as dose-response curves using GraphPad Prism Software. IC<sub>50</sub> values of TAK-228 in cells were calculated using CalcuSyn software and are shown on the right. The figure incorporates data from three replicate experiments. **B**, Effects of TAK-228 on cell-cycle distribution. Cells were treated with TAK-228 (30 nmol/L and 50 nmol/L) for 24 hours. Fixed and propidium iodide-stained cells were analyzed by flow cytometry. The bar chart shows the percentage of cells at different cell stages. **C**, Effects of TAK-228 on 3D cultures. RT4 spheroids or RT4 cells were treated with TAK-228 (50 nmol/L) during 72 hours (viability assay) or 24 hours (Western blot). The viability was determined using CellTiter-Glo luminescent assay (3D) or MTS (2D);  $***, P < 0.001$ . Lysates were analyzed by Western blot for ci-PARP. **D**, Effects of TAK-228 on autophagy. RT4 cells were treated with TAK-228 (50 nmol/L) or everolimus (100 nmol/L) (autophagy-inducer as positive control) in presence or absence of the autophagy inhibitor chloroquine (CLQ) (5  $\mu$ mol/L) for 24 hours. Cyto-ID Green-stained autophagic vesicles were detected by fluorescence microscopy, and representative images of three independent experiments are shown. Cellular extracts were analyzed by Western blot using the indicated antibodies. Values corrected for loading were expressed as fold change of a control condition arbitrarily set to 1.

**Figure 2.**

Molecular effects of TAK-228 on the PI3K/mTOR signaling pathway. **A**, Effects of TAK-228 added *in vitro* on cultured cells. Cells were treated with TAK-228 (50 nmol/L) for 2 and 24 hours. Cellular extracts were analyzed by Western blot analysis using the indicated antibodies. The graphs show the ratio between phosphorylated and total protein in each condition, expressed as fold induction versus control arbitrarily set at 1. Regarding the phospho-4E-BP1 Thr37/46 results, 3 to 4 bands between 20 and 12 kDa are expected to appear, representing the different 4E-BP1 isoforms when phosphorylated at multiple sites. Of note, the upper and lower bands represent the more phosphorylated and unphosphorylated 4E-BP1 isoforms, respectively; \*,  $P < 0.05$ ; \*\*,  $P < 0.01$ ; \*\*\*,  $P < 0.001$ . **B**, Effects of TAK-228 added *ex vivo* to fresh xenografted tumors. Tumors were harvested from mice and sliced. Samples were cultured with or without TAK-228 (RT4 and T24 50 nmol/L, CAL-29 20 nmol/L) during 24 hours and routinely FFPE. Slides were stained with pS6 (Ser235/236). Representative IHC images are shown. Each column represents an effect on the p-S6 expression of the paired control- and TAK-228-treated samples measured as H-score.

These data confirm that TAK-228 inhibits both mTORC1 and mTORC2 in bladder cancer cell lines with underlying alterations in the PI3K/AKT/mTOR pathway.

#### TAK-228 decreases phosphorylation of S6 in tumor samples

CAL-29, RT4, and T24 xenografts were excised and the samples were incubated *in vitro* with TAK-228. Samples were stained for p-S6 (Ser235/236), as a marker of mTORC1 activity. We observed

that TAK-228 inhibits the phosphorylation of S6 in tumor xenograft samples (Fig. 2B) confirming the efficacy of TAK-228 in tumor tissues *in vitro*.

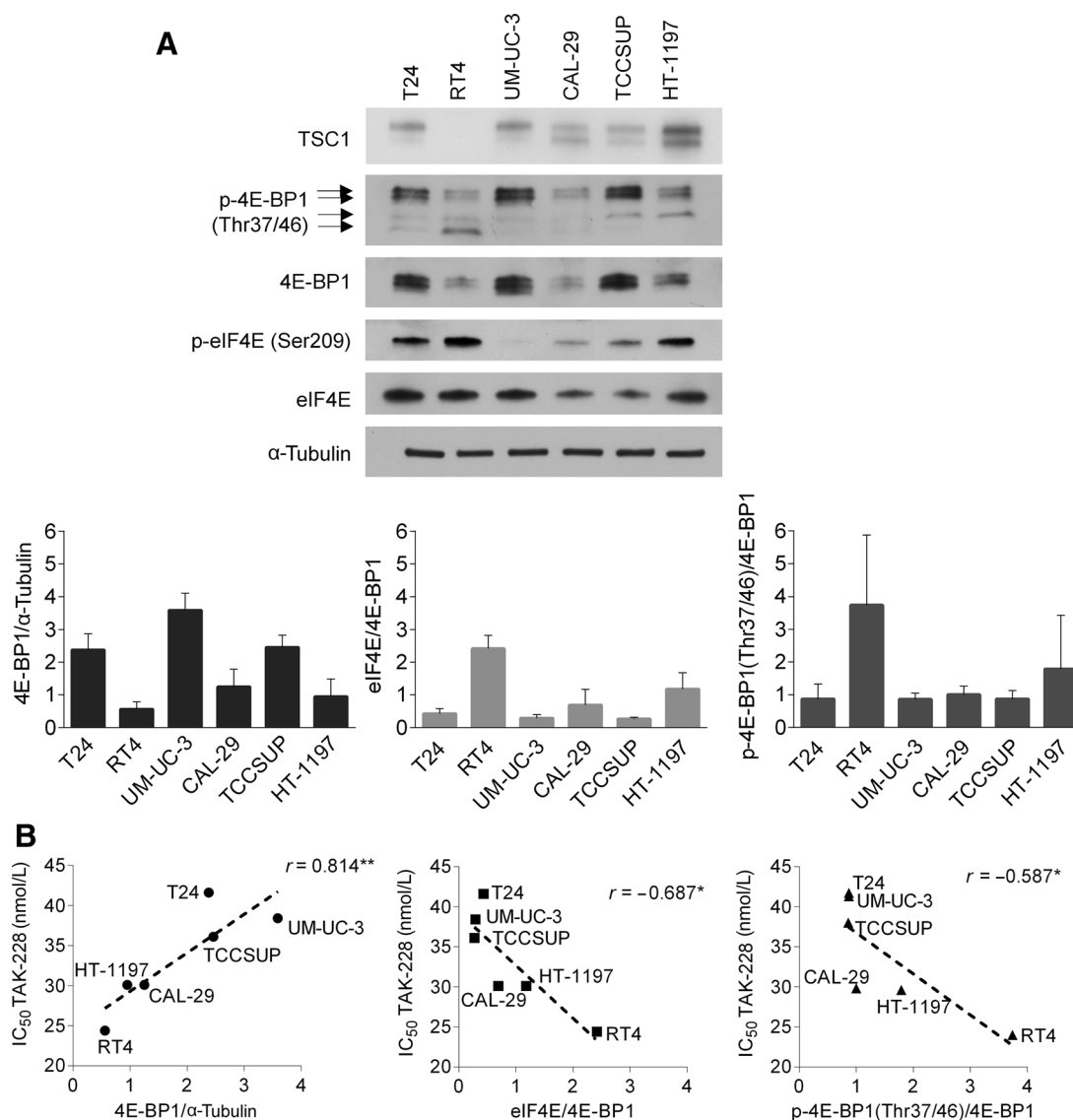
#### Markers of sensitivity or resistance to TAK-228

TSC1 mutations in bladder cancer are associated with increased responses to everolimus in clinical trials (35). Conversely, high 4E-BP1 expression and incomplete dephosphorylation of 4E-BP1

Hernández-Prat et al.

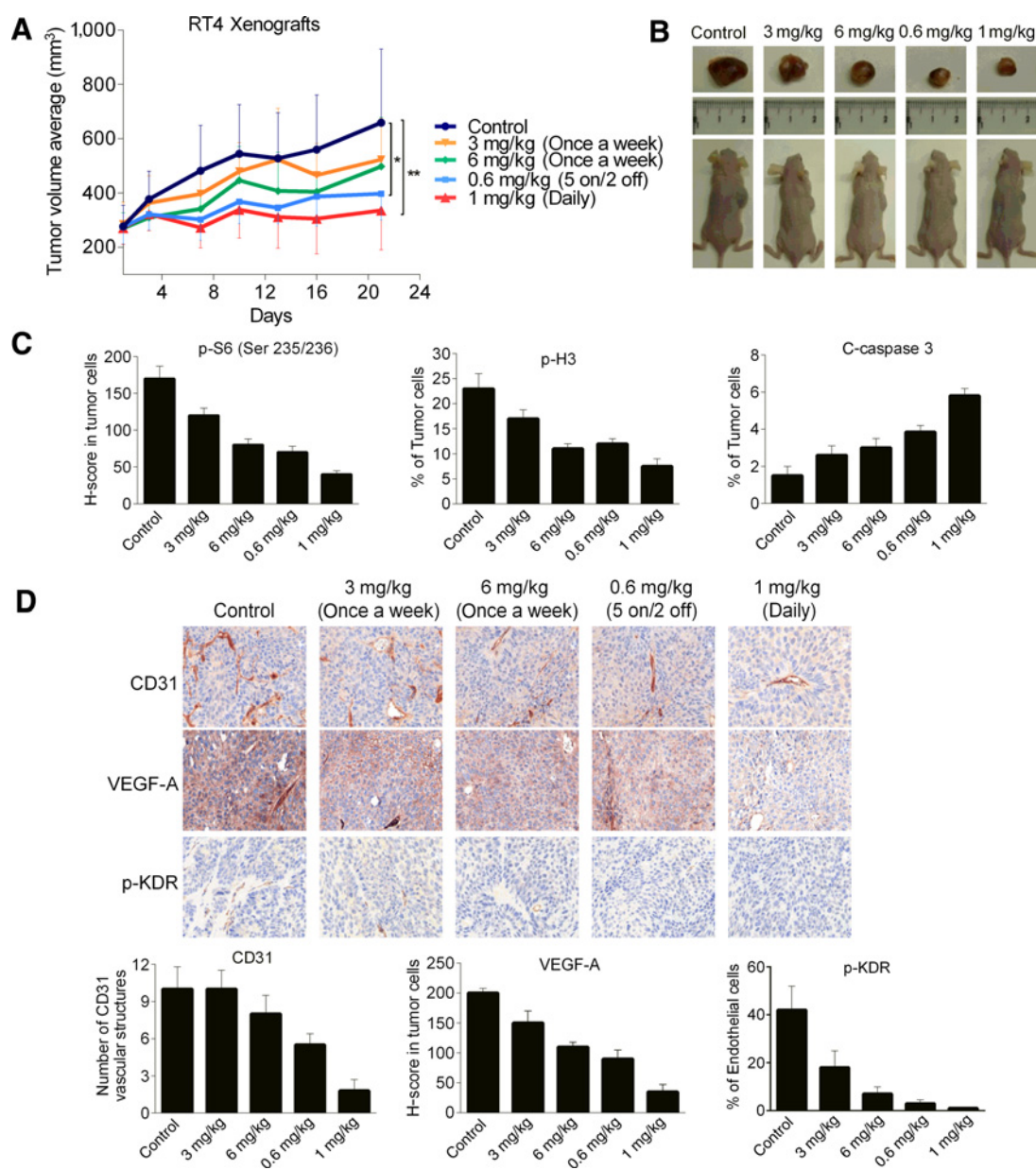
are associated with reduced benefit to dual mTOR inhibitors (36, 37). It has also been described that eIF4E/4E-BP ratio increases in cells with acquired resistance to mTOR inhibitors (38). Hence, we assessed whether any of these markers could predict sensitivity or resistance to TAK-228 in our bladder cancer models. We evaluated these markers in basal cell lysates by Western blot analysis and we determined the correlation between protein expression and IC<sub>50</sub> values for TAK-228. TSC1 expression was present in 5 of the 6 cell lines but was absent in the TSC1-mutated RT4 cell line (Fig. 3A). However, no correlation was found between drug response and TSC1 expression.

Total 4E-BP1 levels were increased in three of the less sensitive cell lines (higher IC<sub>50</sub> values). We found a strong positive correlation between response to TAK-228 and reduced 4E-BP1 levels ( $r = 0.814^{**}$ ), and a moderate negative correlation ( $r = -0.587^*$ ) between p-4E-BP1 (Thr37/46)/4E-BP1 and TAK-228 sensitivity. eIF4E/4E-BP1 ratio also showed a strong negative correlation with drug sensitivity ( $r = -0.687^*$ ; Fig. 3B). These results indicate a potential role of 4E-BP1, eIF4E/4E-BP1, and p-4E-BP1 (Thr37/46)/4E-BP1 as predictive biomarkers of response to TAK-228 in bladder cancer.



**Figure 3.**

Identification of potential biomarkers of sensitivity or resistance to TAK-228. **A**, Baseline expression of PI3K/mTOR-associated pathway components in unstimulated bladder cancer cells. Cells were seeded in 100-mm<sup>2</sup> dishes and left untouched for 48 hours. Cellular extracts were analyzed by Western blot analysis using the indicated antibodies. Three ratios of protein levels were calculated, and the reported values are averages of the three biological replicates; error bars, SEM. **B**, Correlation of protein expression with sensitivity to TAK-228. The correlation between protein expression and TAK-228 drug sensitivity (IC<sub>50</sub> values) was assessed through Spearman rank correlation coefficient ( $r$ ). We considered there was a correlation when  $r$  was close to  $\pm 1$  and the level of significance was lower than 0.05.

**Figure 4.**

*In vivo* effects of TAK-228 on the RT4 xenograft model. **A**, Effects of different schedules and doses. Various doses and schedules of TAK-228 were tested as indicated. Treatment was administered when the average tumor volume reached approximately 200 mm<sup>3</sup> ( $n = 8$  mice/group). A plot of the average tumor volume as a function of time in each treatment group is shown; \*,  $P < 0.05$ ; \*\*,  $P < 0.01$ . **B**, Representative photographs of tumor-bearing mice and the excised tumors. **C**, Effects of TAK-228 on mTORC1, proliferation, and apoptosis. FFPE blocks were prepared from mice tumors. Box plots illustrate the staining results for the indicated antibodies. Each graph is expressed as H-score in tumor cells for p-S6 (Ser235/236) or percentage of stained tumor cells for p-H3 (Ser10) and cleaved caspase-3. **D**, Effects of TAK-228 on angiogenesis. Representative IHC images of xenograft tumor sections stained with the indicated antibodies. Box plots illustrating the staining results or the indicated antibodies. Each graph is expressed as follows: H-score in tumor cells (VEGF-A), percentage of stained endothelial cells (p-KDR), and the number of stained tubular vascular structures within the tumor (CD31). C-caspase 3, cleaved caspase-3.

#### TAK-228 inhibits tumor growth on RT4 xenografts

The RT4 xenograft model was used to test TAK-228 activity *in vivo*. After 21 days of treatment, TAK-228 significantly inhibited tumor growth in both the intermittent low dose (0.6 mg/kg 5 days on/2 days off) and in the continuous low dose (1 mg/kg daily) compared with controls. Tumor sizes in the groups treated once a week with higher doses (3 mg/kg and 6 mg/kg) were not signif-

icantly different from those of the control group (Fig. 4A). Body weight and tumor size measurements were performed twice a week. However, we noticed a slight decrease in weight in the group of mice treated with TAK-228 1 mg/kg, daily (Fig. 4). In further experiments, the drug was administered for 3 consecutive days per week based on the toxicology findings detailed in the Investigator's brochure (IB). No adverse effects were observed within the

Hernández-Prat et al.

dose range and duration of the *in vivo* studies (see Fig. 4B). Significant *in vivo* effects of TAK-228 (at 1 mg/kg daily) versus the control in a T24-xenograft model were observed (Supplementary Fig. S3).

#### TAK-228 suppresses tumor proliferation and angiogenesis

We determined the status of the PI3K/AKT/mTOR pathway activation on excised tumors in each group by IHC. p-S6 was used as a marker of mTORC1 activity. Reduction of total and S6 phosphorylation was observed. The strongest inhibitory effects in tumors were observed in the intermittent low doses (0.6 mg/kg 5 days on/2 days off) and in the continuous low doses (1 mg/kg daily; Fig. 4C). A decrease in the cycling cell marker p-H3 (M phase) was found in all groups. In addition, the number of apoptotic cells (using cleaved caspase-3) increased slightly with treatment. This increment was greater when the animals were treated on a daily basis (Fig. 4C).

Angiogenesis was assessed using three angiogenic markers: CD31 (also known as PECAM-1: Platelet Endothelial Cell Adhesion Molecule-1), VEGF-A, and p-KDR. The number of CD31 vascular structures was significantly reduced with treatment, particularly in the groups treated with TAK-228 at 0.6 mg/kg and 1 mg/kg. VEGF-A levels also decreased when the animals were treated with TAK-228 as did the phosphorylation of KDR receptor (Fig. 4D). In view of these results, we can hypothesize that TAK-228 inhibits *in vivo* tumor proliferation through the inhibition of the PI3K pathway and by reducing angiogenesis.

#### Synergistic effect of TAK-228 and TAK-117 in bladder cancer models

We tested whether TAK-117, a PI3K $\alpha$  inhibitor, could enhance the effects of TAK-228. TAK-117 IC<sub>50</sub> values were obtained for each cell line by MTS assay (Supplementary Fig. S4B). TAK-117 alone significantly inhibited the proliferation of TCCSUP and CAL-29 cell lines and the CAL-29 xenograft (Supplementary Fig. S4A and S4C). These two cell lines have both mutations in the *PIK3CA* but not in the *RAS* genes. These results indicate that TAK-117 might be more active in tumors harboring mutations in the *PIK3CA* gene.

Cells were treated with TAK-228, TAK-117, or the combination of the two drugs. The nature of the interaction observed between TAK-228 and TAK-117 was analyzed with the software CalcuSyn, which uses the median effect method of Chou and Talalay (39). At the IC<sub>50</sub> conditions, the combination showed synergistic activity (CI < 1) in the tested cell lines. For the RT4 and CAL-29 cell lines, this synergistic effect was observed across the majority of the tested conditions. For T24 the synergistic effect was only observed in certain conditions, suggesting that in T24 the combination is less active (Supplementary Table S2). Using automatic counting with Scepter in CAL-29 and RT4 cells, we observed that the combination decreased cell proliferation more strongly than either drug alone (Fig. 5A). In both cell lines, the combination treatment highly reduced S6, AKT, and 4E-BP1 phosphorylation (Western blot), compared with each drug alone (Fig. 5B; Supplementary Fig. S5A). We also investigated the effects of the combination in cell cycle and autophagy. In RT4 cells, both TAK-228 and TAK-117 monotherapy increased G<sub>0</sub>-G<sub>1</sub> phase with further increase when tested in combination (Supplementary Fig. S5B). Higher amounts of LC3-II were observed,

also suggesting that the combination may enhance the activation of autophagy (Supplementary Fig. S5C). Given these findings, we can conclude that the combination acts synergistically *in vitro* in inhibiting cell proliferation, in arresting cell cycle, and in activating autophagy.

#### TAK-117 enhances the effects of TAK-228 in RT4 xenograft model

To validate our *in vitro* results, we analyzed the antitumor effects of the combination in the RT4 xenograft model. Mice were divided into four groups as indicated in Fig. 5C. The combination significantly improved the antitumor effects compared with either of the drugs alone (Fig. 5C). Tumors were excised and stained by pS6 Ser235/236, p-H3, and cleaved caspase-3. A greater reduction in p-S6 phosphorylation and of pH3 was seen with the combination. On the other hand, cleaved caspase-3 expression was increased with the combination as compared with the single agents (Fig. 5D). We observed a decrease in S6 and 4E-BP1 phosphorylation for each drug individually, as well as for the combination. The reduction in proteins levels was slightly higher with the combination, although this was not statistically significant (Fig. 5E). Taking these results together, we confirm our *in vitro* results showing that the combination of TAK-228 plus TAK-117 is more effective in the RT4 xenograft model than each agent alone.

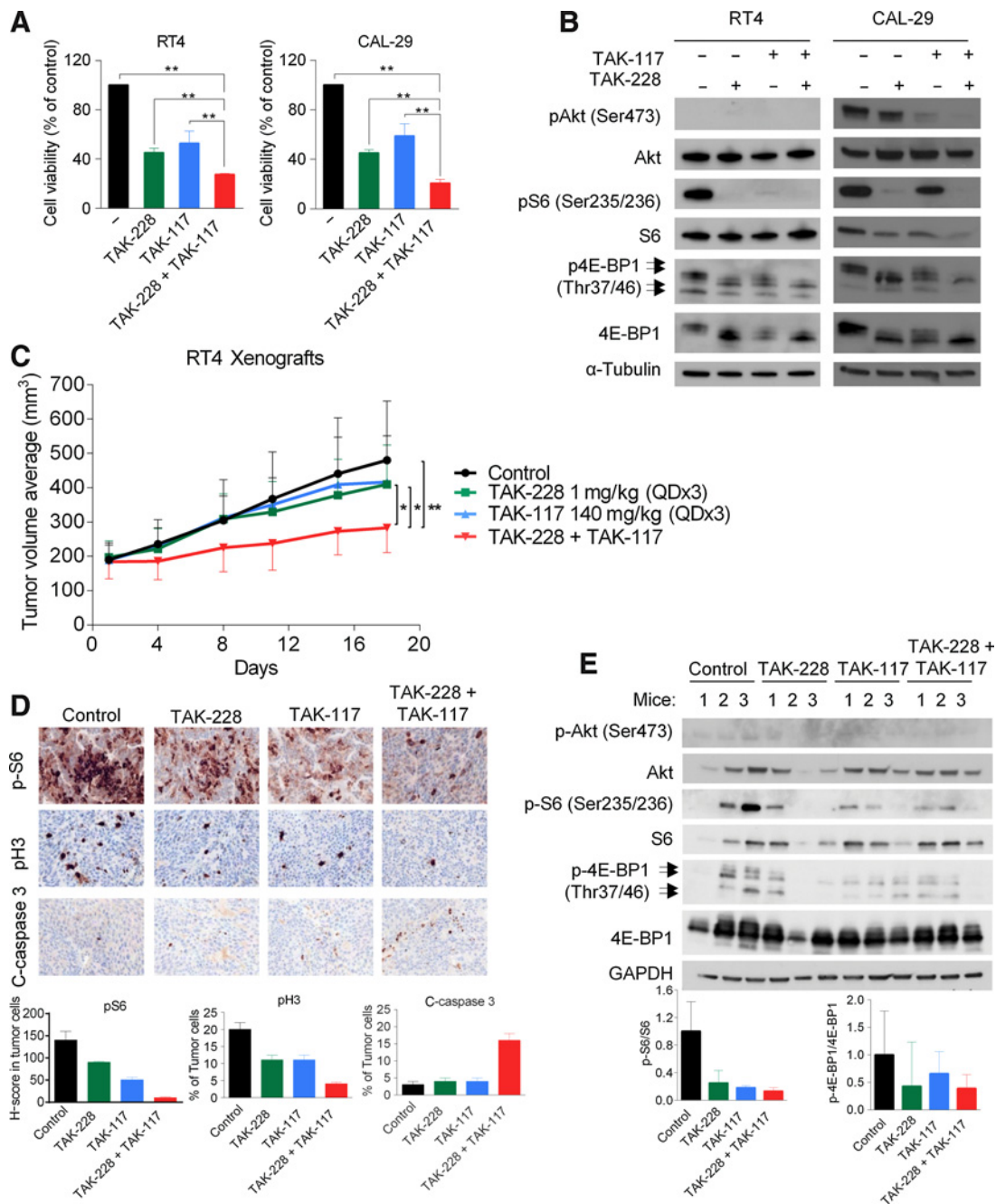
#### TAK-228 enhances the effects of paclitaxel in bladder cancer models

The antiproliferative effect of TAK-228 with paclitaxel given concomitantly or sequentially was tested in four cell lines (Fig. 6A). Concomitant treatment significantly improved the individual effects of each drug alone in RT4, UM-UC-3, and T24 cells (Fig. 6A). Similar effects were observed in CAL-29 cells when compared with TAK-228 alone but not for paclitaxel. Regarding the sequential administration, the combination significantly reduced cell proliferation compared with each individual treatment in all the cell lines (Fig. 6A).

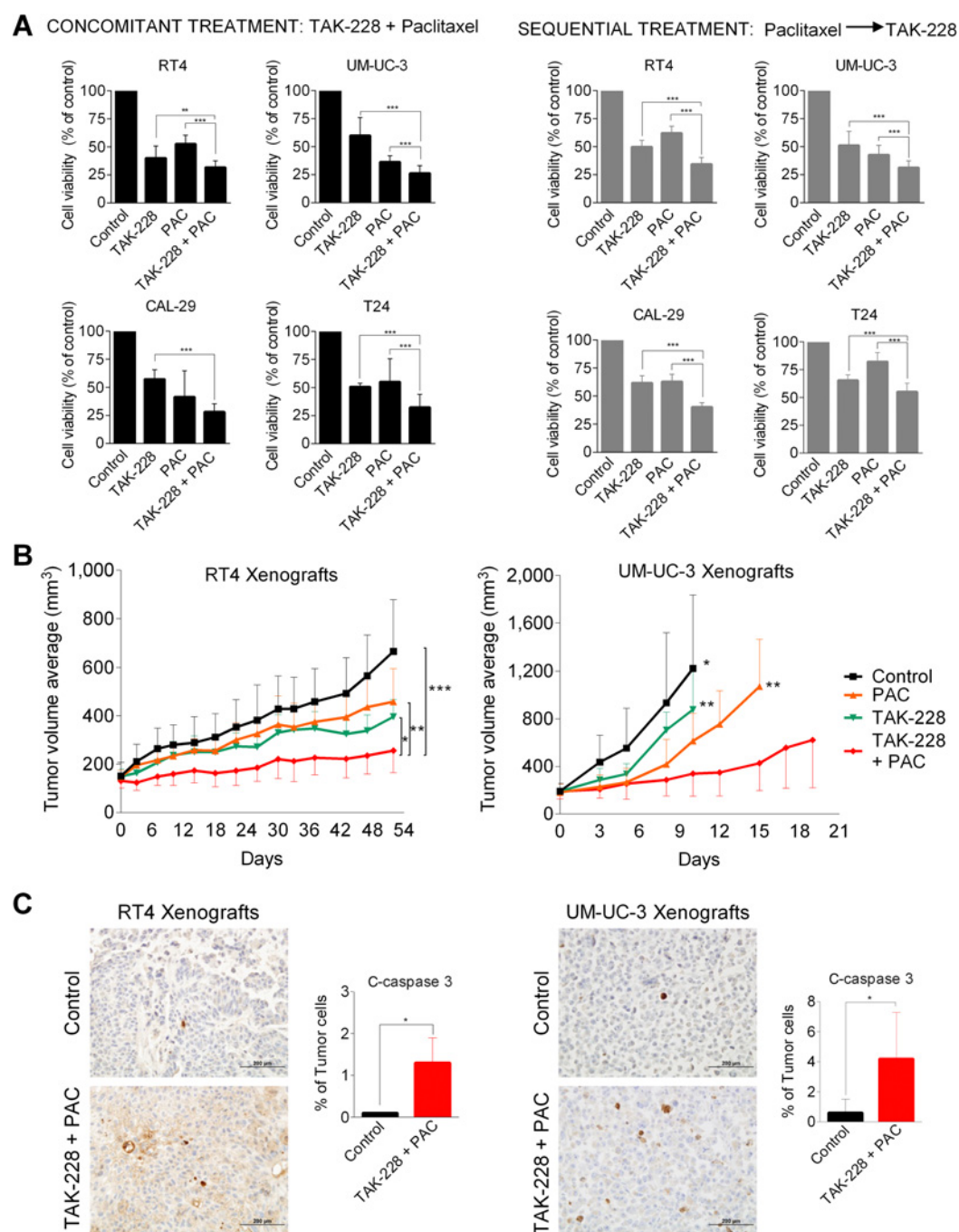
In RT4 cells, TAK-228 and paclitaxel did not enhance the inhibitory effects of TAK-228 on the PI3K/AKT/mTOR pathway at the molecular level (Supplementary Fig. S6A). However, the combination increased G<sub>2</sub>-M phase and decreased G<sub>0</sub>-G<sub>1</sub> phase with respect to the control (Supplementary Fig. S6B). Combination-treated cells showed reduced p62/SQSM1 levels and increased LC3-II levels suggesting that the conversion of LC3-I to LC3-II is greater (more active autophagy) than with any individual drug alone (Supplementary Fig. S6C). Paclitaxel and the combination increased the number of apoptotic cells in 2D cultures (Supplementary Fig. S6D).

#### TAK-228 improves the effects of paclitaxel in xenograft models

Finally, we validated the *in vitro* findings of the combination given sequentially in the RT4 and UM-UC-3 xenografts. Mice were divided into four groups as indicated in Fig. 6B. The combination was associated with a significantly higher reduction on tumor volume compared with each drug alone in RT4 and UM-UC-3 xenograft models (Fig. 6B). We observed that cleaved caspase-3 expression was increased with the combination treatment, suggesting that the combination activates apoptosis (Fig. 6C). Taken together, these results indicate that the addition of paclitaxel to TAK-228 acts in a synergistic manner both *in vitro* and *in vivo*.

**Figure 5.**

Effects of TAK-228 in combination with TAK-117 on bladder cancer models. **A**, Effects of TAK-228 in combination with TAK-117 on cell viability. Cells were plated in 6-well plates and allowed to adhere overnight. Next day, cells were treated with TAK-228 and TAK-117 at the corresponding  $IC_{50}$  values for each drug/cell (RT4: 24.3 nmol/L and 15.7  $\mu$ mol/L; CAL-29: 30.1 nmol/L and 3.5  $\mu$ mol/L, respectively). Cell number was measured using a Scepter 2.0 Cell Counter (Millipore) after 72 hours of treatment. Triplicates were carried out for each concentration, and experiments were repeated three times. The results are expressed as percentages of viable cells in the vehicle-treated control wells; \*\*,  $P < 0.01$ . **B**, Effects of TAK-228 and TAK-117 alone or in combination on the PI3K/mTOR pathway *in vitro*. Cells were treated with TAK-228 and TAK-117 at the corresponding  $IC_{50}$  values, as well as in combination, for 24 hours. Cellular extracts were analyzed by Western blot using the indicated antibodies. **C**, Effects of TAK-228 in combination with TAK-117 *in vivo*. TAK-228 was administered at 1 mg/kg and TAK-117 at 140 mg/kg 3 consecutive days per week. Mice were treated during 3 weeks as indicated. A plot of average tumor volume as a function of time in each treatment group is shown; \*,  $P < 0.05$ ; \*\*,  $P < 0.01$ . **D**, Representative IHC images of xenograft tumor sections. The animals were killed, and the tumors were harvested and FFPE. Pieces were stained for pS6 (Ser235/236), p-H3, and c-caspase 3. Data are representative of independent tumors harvested from 5 mice. Each IHC marker was quantified as described in Fig. 4C. **E**, Western blot images in xenograft tumor lysates. Tumor lysates were analyzed by Western blot using the indicated antibodies. Tumors from 3 mice for each condition were checked. The graphs show the ratio between phosphorylated and total protein in each condition expressed as fold induction versus control arbitrarily set at 1. C-caspase 3, cleaved caspase-3.

**Figure 6.**

Effects of TAK-228 in combination with paclitaxel on bladder cancer models. **A**, Effects of TAK-228 in combination with paclitaxel on cell viability. Cells were plated and allowed to adhere overnight. Cells were treated with TAK-228 and paclitaxel (PAC) at the corresponding IC<sub>50</sub> values for each drug/cell (RT4: 24.3 nmol/L and 5.3 nmol/L; UM-UC-3: 38.4 nmol/L and 3.7 nmol/L; T24: 41.6 nmol/L and 4.7 nmol/L; CAL-29: 30.1 nmol/L and 3.2 nmol/L, respectively). Cells were treated in two ways: concomitantly with TAK-228 and paclitaxel (left) for 72 hours; or sequentially, first with paclitaxel for 24 hours, then adding TAK-228 (right) for 48 hours. Cell viability was measured through MTS. The results are expressed as percentage of viable cells in the vehicle-treated control wells; \*\*,  $P < 0.01$ ; \*\*\*,  $P < 0.001$ . **B**, Effects of TAK-228 in combination with paclitaxel *in vivo*. Mice were divided into four groups ( $n = 8$  mice/group for RT4 xenografts and  $n = 5$  mice/group for UM-UC-3 xenografts): control (PEG400 and water); paclitaxel at 15 mg/kg once per week; TAK-228 at 1 mg/kg 3 times per week; and combination group (sequential paclitaxel followed 24 hours later by TAK-228 at 1 mg/kg, 3 times/week). Mice were treated for 52 days. A plot of average tumor volume as a function of time in each treatment group is shown. For RT4 xenografts: \*,  $P < 0.05$ ; \*\*,  $P < 0.01$ ; \*\*\*,  $P < 0.001$ . For UM-UC-3 xenografts: \*,  $P < 0.05$ , control versus paclitaxel+TAK-228, \*\*,  $P < 0.01$  TAK-228 versus paclitaxel+TAK-228, and \*\*\*,  $P < 0.01$  paclitaxel versus paclitaxel+TAK-228. **C**, Effects of TAK-228 in combination with paclitaxel on apoptosis. Representative IHC images of xenograft tumor sections stained with c-caspase 3. The graph expresses the percentage of stained-tumor cells. C-caspase 3, cleaved caspase-3.

### TAK-228 plus paclitaxel is active *ex vivo* in tumor samples from patients with bladder cancer

We analyzed 6 human bladder cancer explants. In all cases, the combination significantly reduced the S6 phosphorylation compared with the control. In 4 of the 6 samples, the combination

increased cleaved caspase-3 expression and decreased H3 phosphorylation compared with control or monotherapy confirming the efficacy of the combination on human tumor samples (Fig. 7A and B). Representative images of the stained explants are shown in Fig. 7C.

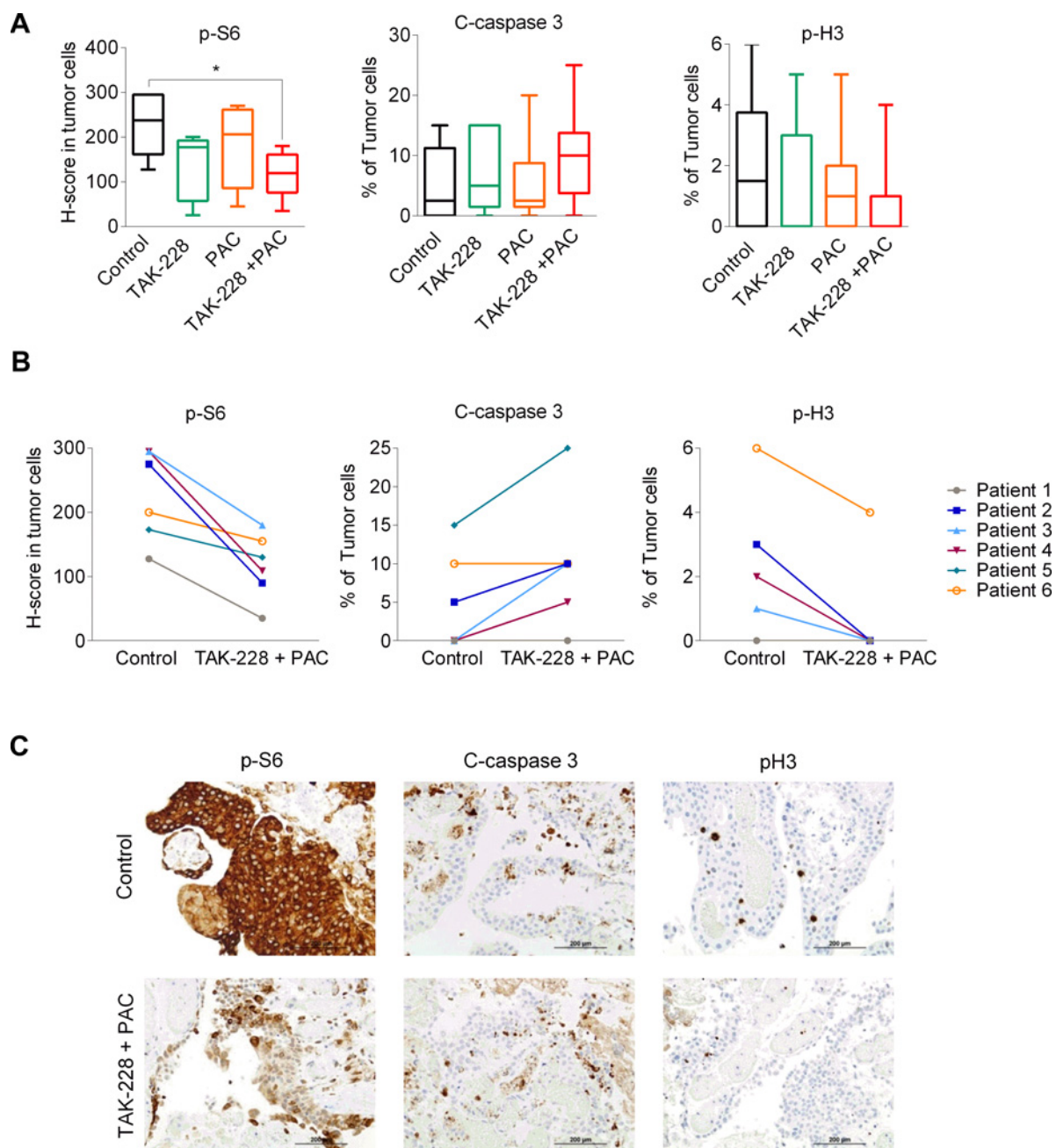


**Figure 7.**

Effects of TAK-228 and paclitaxel added *ex vivo* to fresh bladder cancer explants. FFPE blocks were prepared from bladder tumors samples after 72 hours of treatment with TAK-228 (24.3 nmol/L) and paclitaxel (5.3 nmol/L) alone or in combination. **A**, Graphs showing the percentage of positive cells for active caspase-3 and p-H3, and H-score for p-S6. **B**, Graphs showing the expression of p-S6, active caspase-3, and p-H3 in control condition and after treatment with TAK-228 plus paclitaxel in each patient. **C**, Representative IHC images of control and TAK-228 plus paclitaxel-treated tumors (patient 2) stained with p-S6, active caspase-3, and p-H3 are shown. Scale bar, 50  $\mu$ m/L; \*,  $P < 0.05$ .

## Discussion

Genetic alterations in PI3K/AKT/mTOR pathway have been identified in bladder cancers (10, 11) with a potential for therapeutic intervention. However, the limited overall clinical success of the classical mTORC1 inhibitors in bladder cancer pointed the need to look for better targeted therapies. Many small molecules inhibiting other key nodes in the PI3K/AKT pathway have shown promising activity in bladder cancer preclinical models (17, 18) but were associated with severe adverse effects and failed to show clinical responses in their corresponding clinical trials.

Here, we focused our research on the study of TAK-228, an investigational oral selective ATP-competitive mTORC1/2 inhibitor, as a possible option for treating bladder cancer, in monotherapy, or combined with paclitaxel, or a PI3K $\alpha$  inhibitor. We used bladder cancer cells with different genetic features in the PI3K/AKT/mTOR pathway to mimic the diversity of gene mutations found in patients with bladder cancer. TAK-228 showed good efficacy in all these cells. As expected, the RT4 cell line, which harbors a *TSC1* mutation, was significantly more sensitive to TAK-228 than the other cell lines confirming the positive predictive role of *TSC1* mutation using mTOR inhibitors (35).

However, we found no correlation between *TSC1* protein expression and TAK-228 response in the whole panel of bladder cancer lines, probably due to the different molecular profile of each line. Presently, an open-label, single-arm phase II study (NCT03047213) is evaluating TAK-228 monotherapy activity in patients with advanced bladder cancer with *TSC1* and/or *TSC2* mutations.

To gain insight into the mechanisms of TAK-228, we analyzed some of the cell processes regulated by mTOR showing that TAK-228 induces G<sub>0</sub>-G<sub>1</sub> cell-cycle arrest and activates autophagy. In our study, TAK-228 exhibited antitumor effects by arresting cell cycle and we can speculate that induction of autophagy might have had an additive effect. Despite autophagy having opposing context-dependent roles in cancer with either inducing resistance or sensitizing cells to therapies (40), modulation of autophagy represents a new anticancer strategy with autophagy inducers and/or inhibitors in clinical trials (33).

Remarkably, we did observe *in vivo* induction of apoptosis by TAK-228 but not in 2D traditional monolayer cultures. However, without further analyzing the underlying mechanism, we could demonstrate that apoptosis is indeed activated by TAK-228 in a 3D-spheroids culture setting. Similar contradictory results have been described with other drugs (41).

Our findings show that TAK-228, by inhibiting both mTORC1 and mTORC2 complexes, strongly reduces PI3K/mTOR pathway activation in bladder cancer cells lines and in xenografts. Similar findings have been described in other tumor types (22, 26). mTORC2 has been implicated in promoting invasion and metastasis in bladder cancer (42) suggesting that its inhibition might be of therapeutic relevance. Rapamycin and its analogues have not shown significant activity in bladder cancer partly because of the lack of inhibition of mTORC2. TAK-228 was shown to be superior to everolimus in bladder cancer cell lines confirming that dual inhibition of TAK-228 was more efficiently blocking the PI3K/AKT/mTOR pathway than everolimus. This suggests that TAK-228 might show a better clinical success in patients with bladder cancer.

The antitumor efficacy observed *in vitro* with TAK-228 was confirmed in *in vivo* models. Significant dose-dependent inhibition was seen in monotherapy in the RT4 xenograft and T24 models. Similar *in vivo* effects with TAK-228 had been reported in other tumor types (26, 43). As PI3K/AKT/mTOR pathway plays a key role in angiogenesis (44), we studied angiogenesis markers in tumor samples under TAK-228 treatment. We found that TAK-228 reduced significantly angiogenesis in the treated tumors compared with controls. Taken together, our results indicate that TAK-228 has the potential to be a potent anticancer agent due to its inhibitory effects on cell proliferation, cell cycle, tumor growth, and angiogenesis.

We looked for potential predictive biomarkers in cells with known molecular alterations in PI3K/AKT/mTOR pathway to optimize patient selection in future trials. Low levels of 4E-BP1 and high levels of p-4E-BP1/4E-BP1 and eIF4E/4E-BP1 ratios significantly correlated with cellular responses to TAK-228, indicating a potential role as predictive biomarkers of response and resistance. Other studies have shown that high expressions of p-4E-BP1 or eIF4E are associated with worse prognosis in bladder cancer (45, 46) but none have analyzed their role as predictive biomarkers of response to mTOR inhibitors. Hence, our findings warrant further investigation in prospective biomarker-embedded clinical trials.

Despite the fact that PI3K/AKT/mTOR pathway inhibitors are active anticancer agents, the available clinical data indicate limited efficacy for AKT, mTOR, and PI3K inhibitors administered as single agents. Consequently, it is necessary to define rational combinations based on robust preclinical data of enhanced or synergistic effects. For that reason, we analyzed the role of combining TAK-228 with the PI3K $\alpha$  inhibitor TAK-117 or with paclitaxel with the objective of improving the effects of TAK-228 alone. Importantly, we found that both combinations resulted in synergistic antiproliferative effects in bladder cancer cell lines and in the RT4 xenograft model *in vivo*. Moreover, the molecular inhibition of the PI3K/AKT/mTOR pathway was significantly stronger with the combinations than with each drug alone. The synergistic efficacy of combining an mTOR inhibitor with an AKT or PI3K inhibitor has been studied in multiple cancer types including bladder cancer. Our results on the effect of TAK-228 plus TAK-117 on tumor growth in a bladder cancer xenograft model are confirmatory and extend the conclusions reached by others studies using a chick embryo chorioallantoic membrane (CAM) model (27). Other groups have reported similar results when combining TAK-228 with chemotherapy in other tumors (26, 47) but our report is the first published in two different bladder cancer xenografts.

Moreover, we report for the first time the *ex vivo* activity of TAK-228 in tumor tissues from patients with treatment-naïve bladder cancer.

Taking our results into account, both combination, TAK-228 plus TAK-117 and TAK-228 plus paclitaxel, warrant further evaluation in clinical trials with patients with bladder cancer. Of note, our institution is leading an investigator-initiated phase II study evaluating the efficacy of TAK-228 plus paclitaxel in patients with advanced bladder cancer progressing to prior platinum-based chemotherapy (NCT03745911) including an analysis of predictive tissue biomarkers. The trial is currently open in five Spanish hospitals and enrolment is ongoing. So far, 8 patients with metastatic bladder cancer have been enrolled. This trial will assess whether the preclinical efficacy seen with the combination in our

preclinical model is translated into a clinical benefit in patients with bladder cancer. Moreover, TAK-228 has previously been studied in phase I-II clinical trials, both in monotherapy (NCT01058707) and in combination with paclitaxel (NCT01351350) in several solid malignancies. Both studies showed a favorable toxicity profile with fewer adverse events compared with classic mTOR inhibitors.

Research studies, such as ours, identifying synergistic combinations and predictive biomarkers in preclinical models can help effectively translate the findings into a clinical trial. Those are invaluable tools to increase the probability of success of new-generation targeted agents. As immunotherapy is now an established treatment in bladder cancer, the question is whether there is an opportunity to combine a checkpoint inhibitor with TAK-228. Interestingly, in a preclinical hepatocellular carcinoma model, it was observed that PD-1 overexpression increases both S6 and eIF4E phosphorylation and that TAK-228 plus an anti-PD-1 antibody inhibits proliferation more efficiently than each drug alone (48). On the basis of this observation, the combination of PD-1/PD-L1 inhibitors with TAK-228 warrants further investigation.

In conclusion, our preclinical results indicate that TAK-228 alone or in combination with other therapies might represent a valid therapeutic strategy for patients with advanced bladder cancer and PI3K/AKT/mTOR pathway alterations.

#### Disclosure of Potential Conflicts of Interest

N. Juanpere-Rodero is a consultant pathologist at Synlab and has provided expert testimony for MSD. A. Martínez is an employee at Novartis Pharmaceutical. F. Rojo has received speakers bureau honoraria from Roche, MSD, BMS, Pfizer, Astra Zeneca, Guardant Health, and Agilent, and is a consultant/advisory board member for Roche, BMS, Astra Zeneca, and MSD. J. Bellmunt reports receiving commercial research grants from Takeda, Merck, Astra Zeneca, Genentech, Pfizer, MSD, and BMS, and is a consultant/advisory board member for Merck, Genentech, Astra Zeneca, and Pfizer. No potential conflicts of interest were disclosed by the other authors.

#### References

- Siegel RL, Miller KD, Jemal A. Cancer statistics, 2017. *CA Cancer J Clin* 2017;67:7–30.
- Nadal R, Bellmunt J. New treatments for bladder cancer: when will we make progress? *Curr Treat Options Oncol* 2014;15:99–114.
- Bellmunt J, de Wit R, Vaughn DJ, Fradet Y, Lee JL, Fong L, et al. Pembrolizumab as second-line therapy for advanced urothelial carcinoma. *N Engl J Med* 2017;376:1015–26.
- Balar AV, Galsky MD, Rosenberg JE, Powles T, Petrylak DP, Bellmunt J, et al. Atezolizumab as first-line treatment in cisplatin-ineligible patients with locally advanced and metastatic urothelial carcinoma: a single-arm, multi-centre, phase 2 trial. *Lancet* 2017;389:67–76.
- Robertson AG, Kim J, Al-Ahmadie H, Bellmunt J, Guo G, Cherniack AD, et al. Comprehensive molecular characterization of muscle-invasive bladder cancer. *Cell* 2018;174:1033.
- Bellmunt J, Teh BT, Tortora G, Rosenberg JE. Molecular targets on the horizon for kidney and urothelial cancer. *Nat Rev Clin Oncol* 2013;10:557–70.
- Siefker-Radtke AO, Necchi A, Park SH, Garcia-Donas J, Huddart RA, Burgess EF, et al. First results from the primary analysis population of the phase 2 study of erdafitinib (ERDA; JNJ-42756493) in patients (pts) with metastatic or unresectable urothelial carcinoma (mUC) and FGFR alterations (FGFRalt). *J Clin Oncol* 2018;36 Suppl 15:4503.
- Fruman DA, Rommel C. PI3K and cancer: lessons, challenges and opportunities. *Nat Rev Drug Discov* 2014;13:140–56.
- Laplanche M, Sabatini DM. mTOR signaling in growth control and disease. *Cell* 2012;149:274–93.
- Cancer Genome Atlas Research Network. Comprehensive molecular characterization of urothelial bladder carcinoma. *Nature* 2014;507:315–22.
- Knowles MA, Hurst CD. Molecular biology of bladder cancer: new insights into pathogenesis and clinical diversity. *Nat Rev Cancer* 2015;15:25–41.
- Guertin DA, Sabatini DM. The pharmacology of mTOR inhibition. *Sci Signal* 2009;2:pe24.
- Musa J, Orth MF, Dallmayer M, Baldauf M, Pardo C, Rotblat B, et al. Eukaryotic initiation factor 4E-binding protein 1 (4E-BP1): a master regulator of mRNA translation involved in tumorigenesis. *Oncogene* 2016;35:4675–88.
- Korkolopoulou P, Levidou G, Trigka EA, Prekete N, Karlou M, Thymara I, et al. A comprehensive immunohistochemical and molecular approach to the PI3K/AKT/mTOR (phosphoinositide 3-kinase/v-akt murine thymoma viral oncogene/mammalian target of rapamycin) pathway in bladder urothelial carcinoma. *BJU Int* 2012;110:E1237–48.
- Guba M, von Breitenbuch P, Steinbauer M, Koehl G, Flegel S, Hornung M, et al. Rapamycin inhibits primary and metastatic tumor growth by anti-angiogenesis: involvement of vascular endothelial growth factor. *Nat Med* 2002;8:128–35.
- Chiong E, Lee IL, Dadbin A, Sabichi AL, Harris L, Urbauer D, et al. Effects of mTOR inhibitor everolimus (RAD001) on bladder cancer cells. *Clin Cancer Res* 2011;17:2863–73.
- Sathe A, Gueth F, Cronauer MV, Heck MM, Thalgot M, Gschwend JE, et al. Mutant PIK3CA controls DUSP1-dependent ERK 1/2 activity to confer response to AKT target therapy. *Br J Cancer* 2014;111:2103–13.

#### Authors' Contributions

**Conception and design:** A. Hernández-Prat, O. Arpi, F. Rojo, J. Albanell, R. Brake, A. Rovira, J. Bellmunt

**Development of methodology:** A. Hernández-Prat, A. Rodríguez-Vida, N. Juanpere-Rodero, O. Arpi, S. Menéndez, L. Soria-Jiménez, F. Rojo, R. Brake, J. Bellmunt

**Acquisition of data (provided animals, acquired and managed patients, provided facilities, etc.):** A. Hernández-Prat, A. Rodríguez-Vida, O. Arpi, S. Menéndez, F. Rojo, J. Bellmunt

**Analysis and interpretation of data (e.g., statistical analysis, biostatistics, computational analysis):** A. Hernández-Prat, A. Rodríguez-Vida, N. Juanpere-Rodero, O. Arpi, A. Martínez, F. Rojo, J. Bellmunt

**Writing, review, and/or revision of the manuscript:** A. Hernández-Prat, A. Rodríguez-Vida, N. Juanpere-Rodero, N. Iarchouk, F. Rojo, J. Albanell, A. Rovira, J. Bellmunt

**Administrative, technical, or material support (i.e., reporting or organizing data, constructing databases):** A. Rodríguez-Vida, S. Menéndez, F. Rojo, J. Albanell, J. Bellmunt

**Study supervision:** A. Rodríguez-Vida, A. Martínez, A. Rovira

#### Acknowledgments

The authors would like to thank Dr. Oscar Fornas (Flow Cytometry core facility at Universitat Pompeu Fabra, Barcelona, Spain) and Dr. Xavier Duran (Statistics Unit at Institut Hospital del Mar d'Investigacions Mèdiques, Barcelona, Spain) for technical assistance and comments. We thank Fundació Cellex (Barcelona) for a generous donation to the Hospital del Mar Medical Oncology Department. This work was supported by Instituto de Salud Carlos III (CIBERONC CB16/12/00241, PIE15/00008, PI13/01893, PI16/00112) and Generalitat de Catalunya (2017 SGR 507). Our work is supported by the European Union through the Regional Funding Development Program (FEDER).

The costs of publication of this article were defrayed in part by the payment of page charges. This article must therefore be hereby marked *advertisement* in accordance with 18 U.S.C. Section 1734 solely to indicate this fact.

Received August 31, 2018; revised March 14, 2019; accepted May 28, 2019; published first June 3, 2019.

Hernández-Prat et al.

18. Nawroth R, Stellwagen F, Schulz WA, Stoehr R, Hartmann A, Krause BJ, et al. S6K1 and 4E-BP1 are independent regulated and control cellular growth in bladder cancer. *PLoS One* 2011;6:e27509.
19. Becker MN, Wu KJ, Marlow LA, Kreinest PA, Vonroemeling CA, Copland JA, et al. The combination of an mTORC1/TORC2 inhibitor with lapatinib is synergistic in bladder cancer in vitro. *Urol Oncol* 2014;32:317–26.
20. Bhagwat SV, Gokhale PC, Crew AP, Cooke A, Yao Y, Mantis C, et al. Preclinical characterization of OSI-027, a potent and selective inhibitor of mTORC1 and mTORC2: distinct from rapamycin. *Mol Cancer Ther* 2011; 10:1394–406.
21. Thoreen CC, Kang SA, Chang JW, Liu Q, Zhang J, Gao Y, et al. An ATP-competitive mammalian target of rapamycin inhibitor reveals rapamycin-resistant functions of mTORC1. *J Biol Chem* 2009;284:8023–32.
22. Garcia-Garcia C, Ibrahim YH, Serra V, Calvo MT, Guzman M, Grueso J, et al. Dual mTORC1/2 and HER2 blockade results in antitumor activity in preclinical models of breast cancer resistant to anti-HER2 therapy. *Clin Cancer Res* 2012;18:2603–12.
23. Gokmen-Polar Y, Liu Y, Toroni RA, Sanders KL, Mehta R, Badve S, et al. Investigational drug MLN0128, a novel TORC1/2 inhibitor, demonstrates potent oral antitumor activity in human breast cancer xenograft models. *Breast Cancer Res Treat* 2012;136:673–82.
24. Koo J, Yue P, Gal AA, Khuri FR, Sun SY. Maintaining glycogen synthase kinase-3 activity is critical for mTOR kinase inhibitors to inhibit cancer cell growth. *Cancer Res* 2014;74:2555–68.
25. Hsieh AC, Liu Y, Edlind MP, Ingolia NT, Janes MR, Sher A, et al. The translational landscape of mTOR signalling steers cancer initiation and metastasis. *Nature* 2012;485:55–61.
26. Li C, Cui JF, Chen MB, Liu CY, Liu F, Zhang QD, et al. The preclinical evaluation of the dual mTORC1/2 inhibitor INK-128 as a potential anti-colorectal cancer agent. *Cancer Biol Ther* 2015;16:34–42.
27. Sathe A, Chalaud G, Oppolzer I, Wong KY, von Busch M, Schmid SC, et al. Parallel PI3K, AKT and mTOR inhibition is required to control feedback loops that limit tumor therapy. *PLoS One* 2018;13:e0190854.
28. Young L, Sung J, Stacey G, Masters JR. Detection of mycoplasma in cell cultures. *Nat Protoc* 2010;5:929–34.
29. Canadas I, Rojo F, Taus A, Arpi O, Arumi-Uria M, Pijuan L, et al. Targeting epithelial-to-mesenchymal transition with Met inhibitors reverts chemoresistance in small cell lung cancer. *Clin Cancer Res* 2014;20:938–50.
30. Sabbaghi M, Gil-Gomez G, Guardia C, Servitja S, Arpi O, Garcia-Alonso S, et al. Defective cyclin B1 induction in trastuzumab-emptansine (T-DM1) acquired resistance in HER2-positive breast cancer. *Clin Cancer Res* 2017; 23:7006–19.
31. Barretina J, Caponigro G, Stransky N, Venkatesan K, Margolin AA, Kim S, et al. The Cancer Cell Line Encyclopedia enables predictive modelling of anticancer drug sensitivity. *Nature* 2012;483:603–7.
32. Hoarau-Vechot J, Rafii A, Touboul C, Pasquier J. Halfway between 2D and animal models: are 3D cultures the ideal tool to study cancer-microenvironment interactions? *Int J Mol Sci* 2018;19. doi: 10.3390/ijms19010181.
33. Yang ZJ, Chee CE, Huang S, Sinicrope FA. The role of autophagy in cancer: therapeutic implications. *Mol Cancer Ther* 2011;10:1533–41.
34. Sini P, James D, Chresta C, Guichard S. Simultaneous inhibition of mTORC1 and mTORC2 by mTOR kinase inhibitor AZD8055 induces autophagy and cell death in cancer cells. *Autophagy* 2010;6:553–4.
35. Iyer G, Hanrahan AJ, Milowsky MI, Al-Ahmadie H, Scott SN, Janakiraman M, et al. Genome sequencing identifies a basis for everolimus sensitivity. *Science* 2012;338:221.
36. Ducker GS, Atreya CE, Simko JP, Hom YK, Matli MR, Benes CH, et al. Incomplete inhibition of phosphorylation of 4E-BP1 as a mechanism of primary resistance to ATP-competitive mTOR inhibitors. *Oncogene* 2014; 33:1590–600.
37. Hsieh AC, Nguyen HC, Wen L, Edlind MP, Carroll PR, Kim W, et al. Cell type-specific abundance of 4EBP1 primes prostate cancer sensitivity or resistance to PI3K pathway inhibitors. *Sci Signal* 2015;8:ra116.
38. Alain T, Morita M, Fonseca BD, Yanagiya A, Siddiqui N, Bhat M, et al. eIF4E/4E-BP ratio predicts the efficacy of mTOR targeted therapies. *Cancer Res* 2012;72:6468–76.
39. Chou TC, Talalay P. Quantitative analysis of dose-effect relationships: the combined effects of multiple drugs or enzyme inhibitors. *Adv Enzyme Regul* 1984;22:27–55.
40. Gewirtz DA. The four faces of autophagy: implications for cancer therapy. *Cancer Res* 2014;74:647–51.
41. Fuchs BA, Pruett SB. Morphine induces apoptosis in murine thymocytes in vivo but not in vitro: involvement of both opiate and glucocorticoid receptors. *J Pharmacol Exp Ther* 1993;266:417–23.
42. Gupta S, Hau AM, Beach JR, Harwalker J, Mantuano E, Gonias SL, et al. Mammalian target of rapamycin complex 2 (mTORC2) is a critical determinant of bladder cancer invasion. *PLoS One* 2013;8:e81081.
43. Jiang SJ, Wang S. Dual targeting of mTORC1 and mTORC2 by INK-128 potently inhibits human prostate cancer cell growth in vitro and in vivo. *Tumour Biol* 2015;36:8177–84.
44. Karar J, Maity A. PI3K/AKT/mTOR pathway in angiogenesis. *Front Mol Neurosci* 2011;4:51.
45. Nishikawa M, Miyake H, Behnsawy HM, Fujisawa M. Significance of 4E-binding protein 1 as a therapeutic target for invasive urothelial carcinoma of the bladder. *Urol Oncol* 2015;33:166.
46. Crew JP, Fuggle S, Bicknell R, Cranston DW, de Benedetti A, Harris AL. Eukaryotic initiation factor-4E in superficial and muscle invasive bladder cancer and its correlation with vascular endothelial growth factor expression and tumour progression. *Br J Cancer* 2000;82:161–6.
47. Zhang H, Dou J, Yu Y, Zhao Y, Fan Y, Cheng J, et al. mTOR ATP-competitive inhibitor INK128 inhibits neuroblastoma growth via blocking mTORC signaling. *Apoptosis* 2015;20:50–62.
48. Li H, Li X, Liu S, Guo L, Zhang B, Zhang J, et al. Programmed cell death-1 (PD-1) checkpoint blockade in combination with a mammalian target of rapamycin inhibitor restrains hepatocellular carcinoma growth induced by hepatoma cell-intrinsic PD-1. *Hepatology* 2017;66:1920–33.

# Molecular Cancer Research

## Novel Oral mTORC1/2 Inhibitor TAK-228 Has Synergistic Antitumor Effects When Combined with Paclitaxel or PI3K $\alpha$ Inhibitor TAK-117 in Preclinical Bladder Cancer Models

Anna Hernández-Prat, Alejo Rodriguez-Vida, Nuria Juanpere-Rodero, et al.

*Mol Cancer Res* 2019;17:1931-1944. Published OnlineFirst June 3, 2019.

**Updated version** Access the most recent version of this article at:  
doi:[10.1158/1541-7786.MCR-18-0923](https://doi.org/10.1158/1541-7786.MCR-18-0923)

**Supplementary Material** Access the most recent supplemental material at:  
<http://mcr.aacrjournals.org/content/suppl/2019/06/01/1541-7786.MCR-18-0923.DC1>

**Cited articles** This article cites 47 articles, 14 of which you can access for free at:  
<http://mcr.aacrjournals.org/content/17/9/1931.full#ref-list-1>

**E-mail alerts** [Sign up to receive free email-alerts](#) related to this article or journal.

**Reprints and Subscriptions** To order reprints of this article or to subscribe to the journal, contact the AACR Publications Department at [pubs@aacr.org](mailto:pubs@aacr.org).

**Permissions** To request permission to re-use all or part of this article, use this link <http://mcr.aacrjournals.org/content/17/9/1931>.  
Click on "Request Permissions" which will take you to the Copyright Clearance Center's (CCC) Rightslink site.